Investigation on Energy Director-less Ultrasonic Welding of Thermoplastic to Thermoset Composites

E. Tsiangou[a], S. Teixeira de Freitas[a] ,I. Fernandez Villegas[a]; R. Benedictus[a]

[a] *Structural Integrity and Composites Group, Faculty of Aerospace Engineering, Delft University of Technology, Kluyverweg 1, 2629 HS Delft, The Netherlands*

Keywords: composites, thermosets, thermoplastics, ultrasonic welding, energy director

The exceptionally short heating times achieved with ultrasonic welding make this technique highly promising for joining thermoplastic (TPC) to thermoset (TSC) composites, since it can prevent thermal degradation of the thermoset adherend. A neat thermoplastic coupling layer is co-cured on the surface to be welded as typical procedure to make the TSC "weldable". It is therefore of great interest to investigate whether that coupling layer by itself has the potential to promote heat generation during the ultrasonic welding process with no need for a separate energy director (ED). A possible drawback of this procedure could be that it is more challenging to prevent thermal degradation since the coupling layer is involved in heat generation rather than acting as a thermal barrier. In this research CF/epoxy coupons with a polyetherimide (PEI) coupling layer were welded to compatible CF/TP adherends. The usage of (1) a 0.25 mm thick flat PEI ED and the usage of (2) no ED at all were investigated. Mechanical testing (single lap shear) as well as microscopic analysis of as-welded and tested samples were carried out in this study. Preliminary successful results were obtained for the energy director-less welding process. This research is part of the EFFICOMP project, funded by Horizon2020.

1. Introduction

Welding of thermoplastic composites (TPC) is an efficient bonding technique as it does not require drilling holes, like in the case of mechanical fastening, or the excessive surface treatment necessary for adhesive bonding (Ageorges, Ye, and Hou 2006)(da Costa et al. 2012) . Moreover welding is capable of providing strong joints in a rather fast and clean way. That is why in the past few decades researchers have shown interest in welding not only TPC but also thermoset composites (TSC). The most common way to make TSC weldable is by co-curing a miscible neat TP coupling layer on one surface of the laminate. This TP layer is then used to weld the laminates following the standard TP welding process. A look in the open literature shows two patents filed for bonding TSC with the use of a thermoplastic-rich layer (Jacaruso, Davis, and McIntire 1993)(Jacaruso, Davis, and Mclntire 1994), as well as research papers on application of resistance welding techniques for welding two TSC (R.C. 1994) or for welding a TPC to a TSC (Ageorges and Ye 2006)(Monnard et al. 1997), welding TSC using an oven under vacuum pressure (Hou 2013)(Hou, n.d.)(Paton et al., n.d.), induction welding of TSC to TPC (Schieler and Beier 2016) and ultrasonic welding of TSC to TPC (Villegas and Rubio 2015).

From the authors' point of view, ultrasonic welding is the most interesting technique for welding hybrid composite structures as it is the fastest welding method, with heating times of less than 1 sec. (Villegas et al. 2012)(Villegas and Rubio 2015). That can ensure that thermal degradation of the epoxy matrix is prevented, as it was shown in the research of (Villegas and Rubio 2015). For ultrasonic welding of TPC, a neat TP resin layer which is made from the same material as the TPC matrix, referred to as flat energy director (ED), is placed between the two adherends to be welded to help generate preferential heat at the interface (Villegas et al. 2015).. What is interesting however is that for welding TSC a neat TP layer already exists, i.e. TP the coupling layer co-cured on the TS laminate.

Therefore, the present paper aims at assessing whether it is feasible to ultrasonically weld CF/ Polyetherimide (PEI) to CF/epoxy composites by using only the co-cured TP coupling layer to generate preferential heating at the welding interface during the welding process. PEI was chosen as the material for the coupling layer as it is known to be miscible with most epoxy systems (Lestriez, Chapel, and Gerard 2001). For the feasibility assessment, a comparison between welding with a 0.25mm thick flat ED (ED case) and welding without an extra ED (ED-less case) was made. Firstly, analysis of the interphase between the CF/epoxy and PEI systems was conducted.

Secondly, the mechanical performance of the welded joints was assessed followed by the investigation of the effect of the UW process on the CF/epoxy and CF/PEI adherends and also the morphology of the developed interphase.

2. Experimental Procedure

2.1 *Materials*

In this study, Cetex® CF/PEI (carbon fibre/polyetherimide) with a 5-harness satin fabric reinforcement, manufactured by TenCate Advanced Composites, and T800S/3911 unidirectional CF/epoxy from TORAY, were used. CF/PEI laminates made out of powder-impregnated carbon fabric reinforcement and with a $[0/90]_{3s}$ stacking sequence were consolidated in a hot-platen press at 320 °C and 20 bar for 30 min. The thickness of the consolidated laminates was 1.8mm. Unidirectional CF/epoxy pre-preg was manually laid up in a $[0/90/0/90]_s$ configuration. A 0.06mm-thick neat PEI film (SABIC) , hereafter referred to as "coupling" layer was co-cured to one of the sides of the CF/epoxy laminates. The PEI coupling layer was degreased prior to its application on top of the pre-preg stack. The CF/epoxy laminates with the coupling layer were cured in an autoclave at 180°C and 7 bars for 120 min, according to the specifications of the manufacturer. To ensure flat surfaces on both sides of the laminate, an aluminium caul plate was used on the side of the vacuum bag. The thickness of the CF/epoxy/PEI laminates was 1.92mm CF/PEI and CF/epoxy/PEI adherends with dimensions 25.4mm x 101.6mm were cut from the laminates using a water-cooled circular diamond saw. The CF/PEI adherends were cut with their longitudinal direction parallel to the main apparent orientation of the fibres. The CF/epoxy/PEI adherends were cut with their longitudinal direction parallel to the 0 fibres.

2.2 *Welding process*

Individual samples were welded with a Rinco Dynamic 3000 ultrasonic welder in a single lap configuration , with the overlap being 12.7 mm long and 25.4 mm wide, using the custom-made setup, shown in Fig 1. A cylindrical sonotrode with a 40mm diameter was utilised. To ensure minimum heating times, and hence minimum risk of thermal degradation at an acceptable level of dissipated power, the parameters chosen were 1500N welding force and 86.2µm peak-to-peak vibration amplitude. Solidification force and time were kept constant at 1500N and 4s respectively.

As mentioned in the introduction, two different welding cases were considered in this study: (i) welding with a 0.25mm-thick ED (ED case) and (ii) welding without an extra ED, but only the coupling layer itself (ED-less case). For the ED case displacement-controlled welding was used, as it was shown to provide high-strength welds with minimum scatter (Villegas 2014). The optimum welding displacement was obtained from the feedback data provided by the ultrasonic welder following the procedure defined in (Villegas 2013). For the ED-less case, energy-controlled welding was chosen owing to the fact that the coupling layer was found to act as a thin ED and, as shown in (Palardy and Villegas 2016), thin EDs do not allow displacement-controlled welding. The optimum welding energy was also obtained from the feedback data provided by the ultrasonic welder following the method described in (Palardy and Villegas 2016).

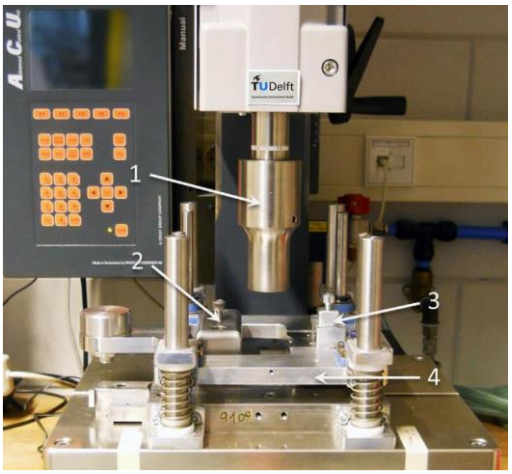

Figure 1. Custom made welding setup. 1: sonotrode, 2: clamp for the lower sample, 3:clamp for the upper sample and 4: sliding platform.(Palardy and Villegas 2016)

2.3 *Testing*

The mechanical performance of the welded samples was assessed by performing single lap shear tests based on the ASTM D 1002 standard in a Zwick 250kN universal testing machine. The apparent lap shear strength (LSS) of the joints was calculated as the maximum load divided by the overlap area. Five specimens were welded per welding case to determine the average LSS. Naked eye observation, optical microscopy (Zeiss Axiovert 40 optical microscope) and scanning electron microscopy (SEM, JEOL JSM-7500F scanning electron microscope) were used for fractographic analysis of the welded joints and to analyse the interphase between epoxy and PEI. To observe the interphase the samples were etched with N-Methyl-2-pyrrolidone (NMP) solvent to provide a better contrast. Lastly, RAMAN spectroscopy (Renishaw inVia Raman microscope) was utilised to measure the thickness of the interphase and to analyse its composition.

3. Results and discussion

3.1 CF/epoxy-PEI interphase

Figure 2 shows the optical micrograph of an etched CF/epoxy sample with the PEI co cured coupling layer. A darker grey area is seen in between the lighter grey epoxy and the PEI, indicating that the two materials actually formed an interphase, even visible by optical microscopy. Note that the bigger particles in the epoxy side are toughening particles, common in the latest prepreg systems. A closer look of the interphase is presented in Figure 3. The interphase is formed by spheres that decrease in size towards the PEI coupling layer. Those spheres are formed in the epoxy system while the co-curing process takes place and during which the epoxy is acting as a solvent of the PEI, with PEI molecules diffusing in the epoxy and vice versa. Diffusion of the epoxy molecules in the PEI is explained by the reduction in thickness of the pure PEI coupling layer, which is 0.06mm before the curing process and less than 0.05mm afterwards. This formation mechanism is known in literature as nucleation and growth (Ougizawa and Inoue 2014). Once the curing process is completed, a gradient concentration of the two polymers is developed, leading to the final morphology seen in Figure 3. The gradient interphase can be seen in the RAMAN spectroscopy concentration graph shown in Figure 4, in which a gradient transition from colour white, which represents the pure epoxy, to colour black, which represents the pure PEI, is observed. It is interesting to note that, as seen in Figure 3, there is a clean cut at the epoxy-interphase boundary instead of a smooth transition. Reasons for this behaviour need to be investigated further.

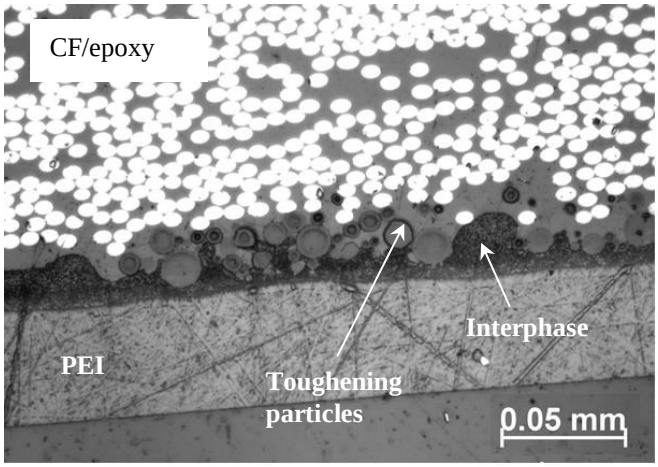

Fig. 2 Optical micrograph of etched CF/epoxy sample with the co-cured PEI coupling layer

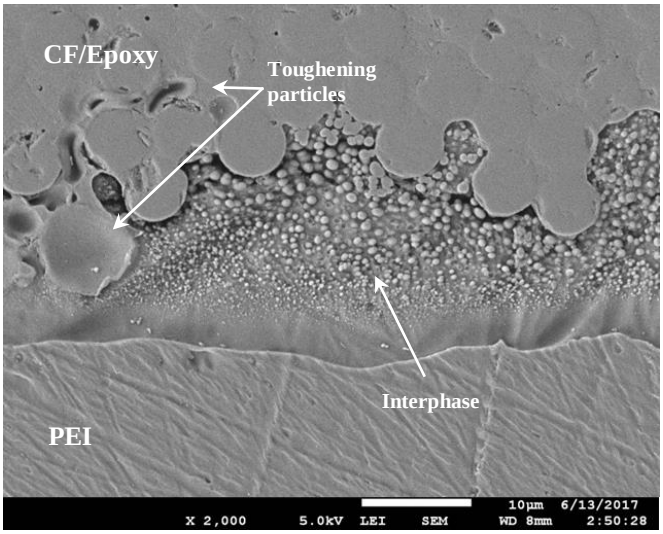

Fig 3. SEM image of the T800S/3911-PEI interphase

The toughening particles were found to affect the formation of the interphase, as shown in Figure 5, in areas where particles are present the interphase has a thickness of just a few µm whereas in particle-free regions the interphase zone is more extended and can reach a width of approximately 25 µm, measured via a RAMAN spectroscopy concentration graph like the one presented in Figure 4.

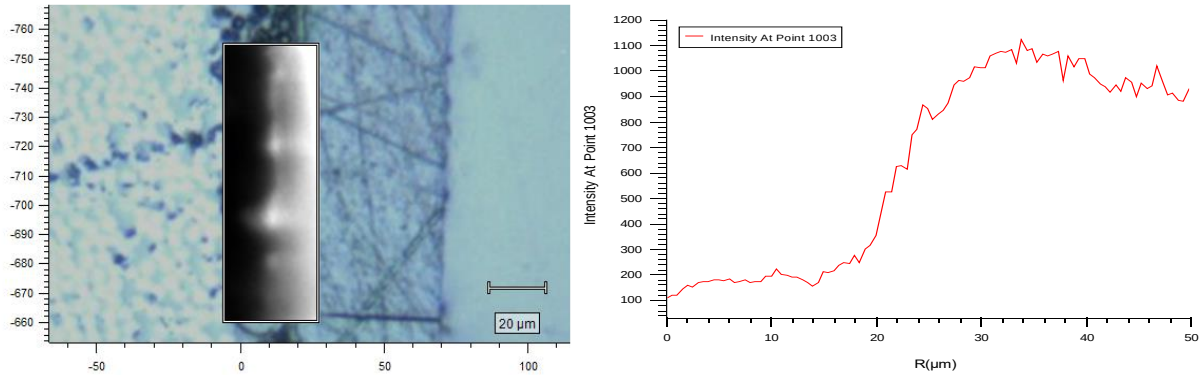

Fig.4 RAMAN spectroscopy image with black color representing the epoxy material and white the PEI (left) and RAMAN spectroscopy concentration graph (right). X axis represents the width of the scanned area and Y axis the intensity of a charachteristic PEI spectrum peak.

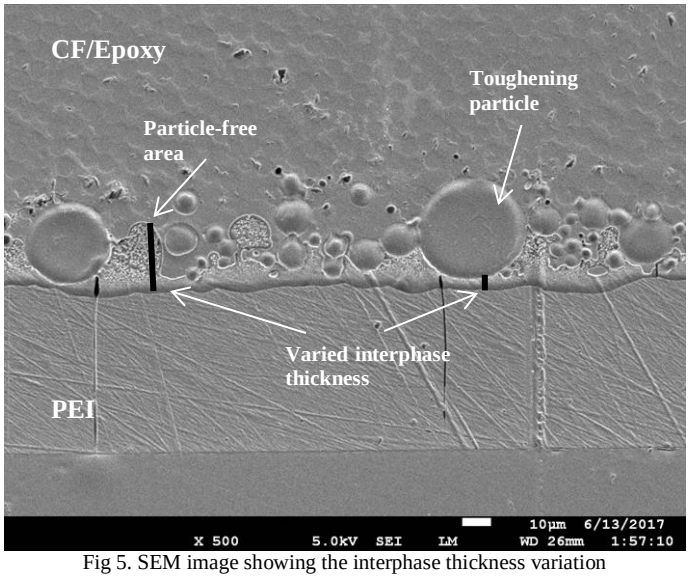

Fig 5. SEM image showing the interphase thickness variation

3.2 Welded joints

The average LSS for both welding cases and corresponding scatter (standard deviation) are presented in figure 6. The average LSS for the ED-less case is 24% lower than the average LSS for the ED case. The scatter of the LSS values yielded by the ED-less welds is high. These two observations can be explained by observing the fracture surfaces of the ED-less welds, three of which are shown in figure 7. The lower LSS of the ED-less welds can be explained by the incomplete welding of the overlap area resulting in unmolten areas, contrary to the fully welded areas obtained in the ED welds. Moreover, the amount and location of the welded areas varied from sample to sample, explaining the high scatter for the ED-less case.

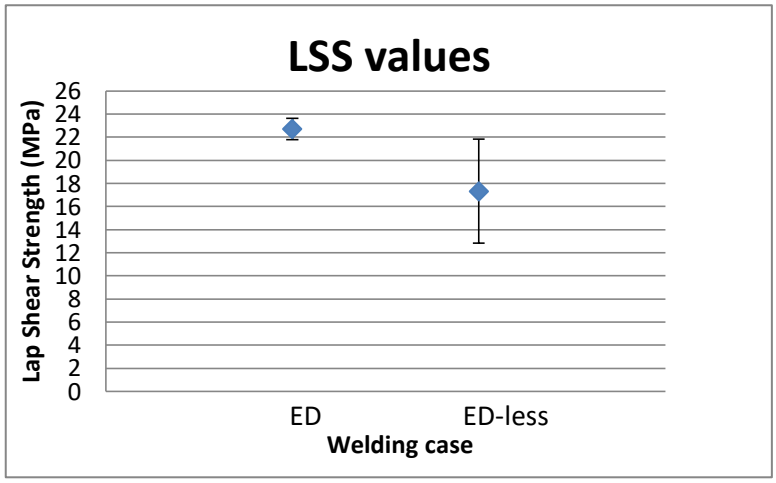

Fig 6. LSS of ED and ED-less welding cases

Fig 7. Fracture surfaces obtained for the ED-less welding case with the same welding parameters.

To determine the failure mechanisms taking place in both welding cases a closer inspection of the fracture surfaces was performed. Figure 8a shows a representative ED-less fracture surface. Inspection revealed: (i) failure within the PEI coupling layer and (ii) first-ply failure in the CF/epoxy/PEI laminate without being clear, however, whether the latter occurs at the interphase-epoxy boundary or within the interphase. Flakes and porosity could be seen in the areas where failure occurred within the coupling layer. This finding is consistent with results on thin PEI energy directors presented by (Palardy and Villegas 2016) and might be an indication of thermal degradation of the coupling layer, as the lack of flow of the molten PEI and the generated hot spots does not help getting a uniform temperature field. Further investigation is required however to draw definite conclusions on the thermal degradation matter.

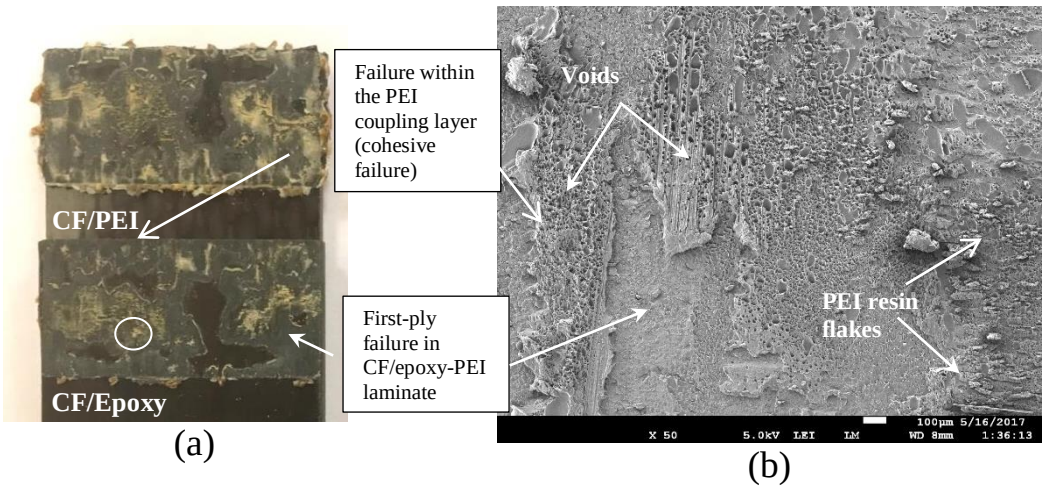

Fig 8. (a) Representative fracture surface of ED-less welded sample and (b), corresponding SEM images circled in (a)

The failure mode of the ED case samples is different than the ED-less ones. In the ED case failure is characterized by i) first-ply failure in the CF/PEI with fibre/matrix debonding (Figures 9a, b) and ii) first-ply failure in the CF/epoxy. In this case, detailed examination of the fracture surfaces revealed that the first-ply failure in the CF/epoxy laminate was a combination of failure within the interphase and in the epoxy resin itself (Figures 9c,d), whereas for the ED-less case there are no such indications. One potential reason why the specimens seem to fail at the interphase could be that the welding process has some sort of weakening effect on it, although this needs to be further investigated. Lastly, no signs of porosity or flakes are visible, indicating that probably no thermal degradation has occurred to any of the adherends or the ED, contrarily to what was seen in the ED-less case.

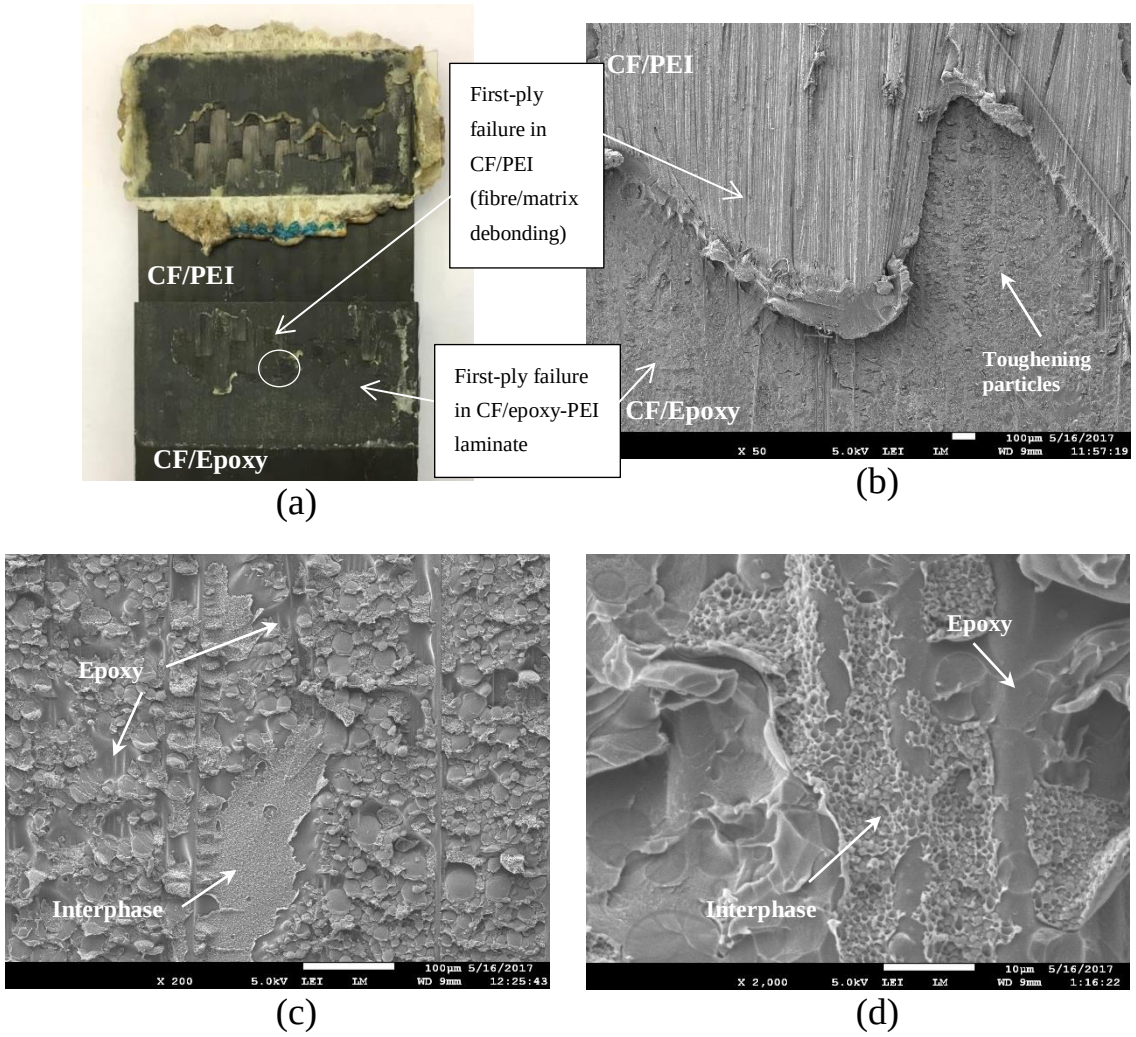

Fig 9. (a) Representative fracture surface of ED welded sample and (b) corresponding SEM image circled in (a), (c) and (d) SEM images of failure in the CF/epoxy

To have a complete understanding of the effect of the UW process on the welds, a cross section study of the welded joints was performed. Figure 6a presents a clean cross section micrograph for the ED case, which shows no porosity in the vicinity of the weld line and hence absence of visible signs of thermal degradation as expected from the selection of the welding parameters and previous results in (Villegas and Rubio 2015). The ED-less case shows however abundant porosity in the weld line, as already seen on fracture surfaces (Figure 6b). Interesting to note that no porosity can be found in the CF/epoxy composite. A potential reason can be the severe through-the-thickness temperature gradient during ultrasonic welding owing to very localised heat generation and to very short heating times. Some voids can however be seen in the CF/PEI adherend. Further research will provide more insight on this matter.

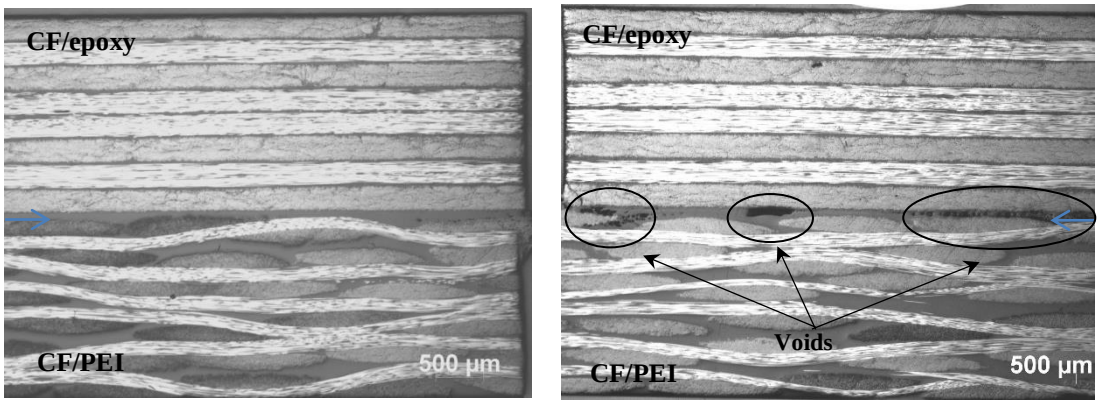

Fig 10. Cross-sectional micrographs of as welded specimen for the ED (left) and ED-less (right) welding case. Blue arrows indicate the interface.

Finally, to explain why failure at the interphase was observed in the ED case, SEM inspection of as welded specimens was performed (Figure 11). The SEM images seem to indicate that the welding process does not have an effect in the interphase for either of the welding cases, with the fine distribution of the epoxy spheres remaining intact.

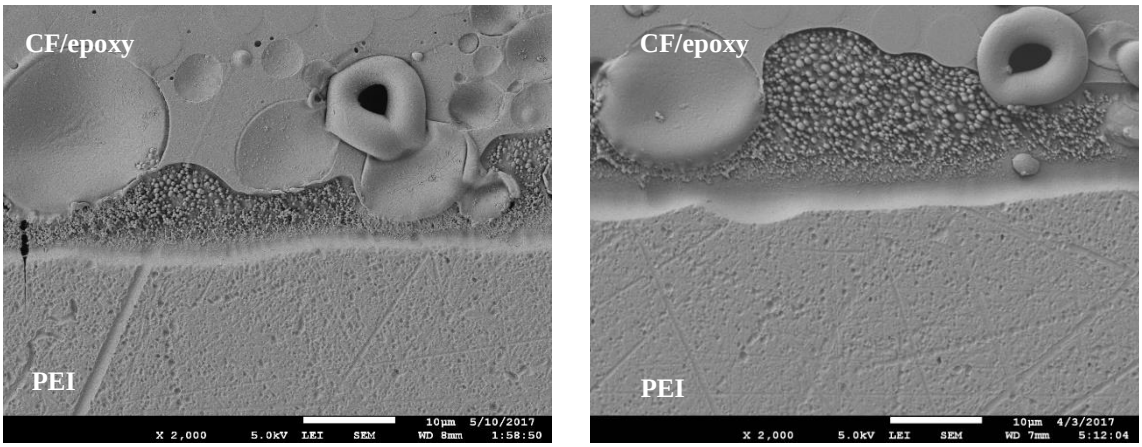

Fig 11. SEM images of as welded specimens for the ED case (left) and ED-less case (right)

Conclusions

In this paper, experimental assessment of the feasibility of ED-less ultrasonic welding of TPC to TSC was presented. Two welding cases were considered, welding with a 0.25mm thick ED and welding without an extra ED. Analysing the results presented in the previous section led to the following observations:

- A gradient interphase is formed between the T800S/3911 epoxy and polyetherimide (PEI) systems by the nucleation and growth mechanism, evident by the existence of epoxy spheres in the PEI. The interphase morphology could be resolved via SEM of samples etched with NMP.
- The thickness of the interphase can be measured using RAMAN spectroscopy. The thickness of the interphase varies between a few nm and approximately 25µm. Thickness variations are most likely due to the presence of TP toughening particles and carbon fibres.
- For both ED and ED-less welding cases the welding process does not appear to affect the initial interphase morphology. However, for the ED-less welding case thermal degradation signs are present in the PEI-rich welding line contrary to the ED case where no signs are visible. Interestingly, no thermal degradation in the epoxy was observed.
- For 0.25 mm ED, fully welded areas were observed. The failure mode was mostly governed by first ply failure in the CF/PEI and first ply failure in the CF/epoxy adherend, with clear signs of failure both at the interphase and the epoxy itself. The LSS is 22.7±0.9 MPa.
- For no ED, first ply failure in the CF/PEI adherend does not occur. Failure mostly happens in the PEI coupling layer and in the first ply of the CF/epoxy but it is not clear whether the latter occurs at the interphase-epoxy

boundary or within the interphase. The amount of welded areas is not consistent, but in all cases 100% welded area were not achieved. Consequently, LSS is lower than in the ED case and with a higher deviation, i.e. 17.3±4.5MPa.

Acknowledgements

This research is part of the EFFICOMP project, funded by Horizon2020.

Bibliography

Ageorges, C, and L Ye. 2006. "Resistance Welding of Thermosetting Composite / Thermoplastic Composite Joints." *Advanced Materials* 32 (2001).

Ageorges, C, L Ye, and M Hou. 2006. "Advances in Fusion Boding Techniques for Joining Thermoplastics Materials Composites: A Review" 32 (2001). http://ac.els-cdn.com/S1359835X00001664/1-s2.0-S1359835X00001664-main.pdf?_tid=4a82ae48-eb1b-11e3-8fe4-00000aab0f01&acdnat=1401798999_d1ae1e214550a9b8f7b754bdd7fd8124.

Benatar, A. 2014. "Ultrasonic Welding of Plastics and Polymeric Composites." In *Power Ultrasonics: Applications of High-Intensity Ultrasound*. doi:10.1016/B978-1-78242-028-6.00012-0.

da Costa, Anahi Pereira, Edson Cocchieri Botelho, Michelle Leali Costa, Nilson Eiji Narita, and Jos?? Ricardo Tarpani. 2012. "A Review of Welding Technologies for Thermoplastic Composites in Aerospace Applications." *Journal of Aerospace Technology and Management* 4 (3): 255–65. doi:10.5028/jatm.2012.04033912.

Fernandez Villegas, I., B. Valle Grande, H.E.N. Bersee, and R. Benedictus. 2015. "A Comparative Evaluation between Flat and Traditional Energy Directors for Ultrasonic Welding of CF/PPS Thermoplastic Composites." *Composite Interfaces* 22 (8): 717–29. doi:10.1080/09276440.2015.1053753.

Fernandez Villegas, Irene, and Pablo Vizcaino Rubio. 2015. "On Avoiding Thermal Degradation during Welding of High-Performance Thermoplastic Composites to Thermoset Composites." *Composites Part A: Applied Science and Manufacturing*. doi:10.1016/j.compositesa.2015.07.002.

Grewell, David A., Avraham Benatar, and Joon B. Park. 2003. *Plastics and Composites Welding Handbook*. Munich: Hanser Gardner Publications.

Hou, Meng. n.d. "Thermoplastic Adhesive for Thermosetting Composites." doi:10.4028/www.scientific.net/MSF.706-709.2968.

———. 2013. "Fusion Bonding of Carbon Fiber Reinforced Epoxy Laminates." *Advanced Materials Research* 626. doi:10.4028/www.scientific.net/AMR.626.250.

Jacaruso, Gary J., Geoffrey C. Davis, and Allen J. McIntire. 1993. Method of Making Thermoplastic Adhesive Strip for Bonding Thermoset Composite Structures, issued 1993.

Jacaruso, Gary J., Geoffrey C. Davis, and Allen J. Mclntire. 1994. Bonding of Thermoset Composite Structures, issued 1994.

Lestriez, Bernard, Jean-Paul Chapel, and Jean-Francois Gerard. 2001. "Gradient Interphase between Reactive Epoxy and Glassy Thermoplastic from Dissolution Process, Reaction Kinetics, and Phase Separation Thermodynamics." *Macromolecules*, 1204–13.

Monnard, Veronique, P-e Bourban, J.-A. E Månson, Douglas A Eckel, John W Gillespie, Stephen H McKnight, and Bruce K Fink. 1997. "Processing and Characterization of Welded Bonds between Thermoset and

Thermoplastic Composites." In *SAMPE EUROPE*.

Ougizawa, Toshiaki, and Takashi Inoue. 2014. *Morphology of Polymer Blends*. doi:10.1007/978-94-007-6064-6.

Palardy, Genevieve, and Irene F. Villegas. 2016. "On the Effect of Flat Energy Directors Thickness on Heat Generation during Ultrasonic Welding of Thermoplastic Composites." *Composite Interfaces* 6440 (August): 1–12. doi:10.1080/09276440.2016.1199149.

Paton, Rowan, Meng Hou, Andrew Beehag, and Paul Falzon. n.d. "A Breakthrough in the Assembly of Aircraft Composite Structures." In *25th International Congress of the Aeronautical Sciences*, 1–8.

R.C., Don. 1994. "Application of Thermoplastic Resistance Welding Techniques to Thermoset Composites." *Annual Technical Conference Society of Plastics*.

Schieler, Oliver, and Uwe Beier. 2016. "Induction Welding of Hybrid Thermoplastic-Thermoset Composite Parts" 9 (1): 27–36. doi:10.14416/j.ijast.2015.10.005.

Villegas, I. F. 2013. "In Situ Monitoring of Ultrasonic Welding of Thermoplastic Composites through Power and Displacement Data." *Journal of Thermoplastic Composite Materials*, 66–85. doi:10.1177/0892705712475015.

Villegas, Irene Fernandez. 2014. "Strength Development versus Process Data in Ultrasonic Welding of Thermoplastic Composites with Flat Energy Directors and Its Application to the Definition of Optimum Processing Parameters." *Composites Part A: Applied Science and Manufacturing*. doi:10.1016/j.compositesa.2014.05.019.

Villegas, Irene Fernandez, Lars Moser, Ali Yousefpour, Peter Mitschang, and Harald E N Bersee. 2012. "Process and Performance Evaluation of Ultrasonic , Induction and Resistance Welding of Advanced Thermoplastic Composites." *Journal of Thermoplastic Composite Materials* 26 (8): 1007–24. doi:10.1177/0892705712456031.